IOP Conf. Series: Materials Science and Engineering **454** (2018) 012182 doi:10.1088/1757-899X/454/1/012182

Synthesis of Alumina Sub-Microstructure Particles Using In-House Methods

Almahdi R. Rabia[1], Abdul Haqi Ibrahim[1], Nik Noriman[1], Sam Sung Ting[3], Tijjani Adam[2]

[1]School of Environmental Engineering, Universiti Malaysia Perlis, Kompleks Pusat Pengajian Jejawi 3, 02600 Arau, Perlis, Malaysia
[2]Faculty of Engineering Technology, Kampus Uniciti Alam Sg. Chuchuh, 02100 Padang Besar, Universiti Malaysia Perlis (UniMAP)
[3]School of Material Engineering, Universiti Malaysia Perlis, Kompleks Pusat Pengajian Jejawi 3, 02600 Arau, Perlis, Malaysia

Abstract. The paper reported novel synthesis of alumina AlxOy Sub-Microstructure Particles Using In-House Methods. The structure was synthesized from aluminium oxide by in-house prepared method. The synthesis was performed using caustic soda (NaOH) assisted, pure aluminium was dissolved in pre-prepared solution of DI, H2O4, NaOH. AlxOy was prepared in crucible via 5 different pH solutions of DI, H2O4, NaOH. The pure aluminium powder was prepared from 2 NaAl(OH)4. The process passed through three reactions; Oxidation Al(OH)y, evaporation AlxOy, and dissolution 2NaAl(OH)z: Uniformly distributed activated was synthesis with the average diameter of the alumina AlxOy sub-microstructures between 10.34 to 40.2µm were realised. The prepared, activated alumina was tested against three columns of 1,260 cm3, 675 cm3 and 525 cm3 with 27 samples of different content of activated. It was found, all the three columns show to total reduction of the lead from the water with increase content of activated alumina.

1. Introduction

The entire performance of activated in application such as water treatment is largely depending on it aspect ratio which is directly related to the microstructure integrity [1]. However, activated alumina as the size shrinkages the presence of minutes impurities greatly affect entire integrity of the materials, problems such a crack generated by the effects of stresses caused by the difference between the coefficients of thermal expansion of the original materials and impurities is causing a serious concern [2]. It is necessity to have simple but powerful techniques to synthesis activated alumina of high aspect ratio without any damage [3]. Several researchers have proposed the activated alumina potential on the lead Pb removal from water [4]. However, most of these researchers bought the activated from manufacturers. The purchasing of activated alumina is making the treatment process costly and, in most cases, the real absorption mechanism cannot be fully revealed [5]. For these, the study proposed cheap techniques of synthesising activated alumina. Moreover, Aluminium oxide derived materials have attracted the attention of research community especially activated alumina due several advantages such as its thermal stability, novel chemical, physical mechanical and optical properties [6]. It is tremendously have shown potential benefit over several composite and ceramics materials [7]. It has widely been used in automation industries, aerospace, due to its lightweight and good mechanical strength [7]. Currently, the materials used in various applications are not meeting the required properties [8]. Thus, the possibility replacing current materials by using alumina showing a

positive affirmation, as the activated alumina have been used in many applications such water treatment, land field treatment and odour reduction such reduction of hydrogen sulphide [9].The use of alumina as a substitute for various is only depend on its samples formulations and added materials such allow[10]. The materials have shown potential of replacing ceramic materials by adding porcelain during processing has been in proposed by several researchers [11-13]. The materials have shown promising properties such chemical and mechanical characteristics [14]. Alumina is a stable material with very linear shrinkage [15]. It have come with different crystal shape and it crystal shape is paramount determining several factor to altered its mechanical especially redial strength, the addition of additive such porcelain it enhances its high Young's modulus which directly determine its strength [16] The pure alumina have embedded different, it have been process and synthesised with different materials crystals and produced size of different ranges from small up to larger structure with an average particle diameter of ~ 10 μm. However, this comes with some disadvantages because as it becomes smaller the linear shrinkages is no more obtainable [17 Another important aspect that is characteristic of the microstructure of alumina as the size shrinkages the presence of minutes impurities greatly affect entire integrity of the materials, problems such a cracks generated by the effects of stresses caused by the difference between the coefficients of thermal expansion of the original materials and impurities have been reported [18]. The major problem of getting smaller distributed activated alumna is the techniques involved [19]. When careful consideration techniques, the problem of crack can be avoided with the substitution of the alumina the proposed in-house processing methods proposed by this study [20].

2. Materials and Method

In order to synthesize the alumina Al_xO_y Sub-Microstructure, pure aluminium is necessary, therefore the samples of aluminum standard powder of different orientation were purchase in well know company of Meridian World Sdn. Bhd, which is one of the environmental service providing company at Sungai Petani, Kedah Darul Aman, Malaysia. Pure aluminum (grade A 100% pure), reacted, at room temperature, with a aqueous NaOH in a reactor to produce a solution of sodium aluminate ($NaAlO_2$). This solution was passed through filter paper and the clear filtrate was neutralized with H_2SO_4, to pH 6, 7 or 8, resulting in the precipitation of a white gel, Al(OH)3·XH2O. The paper reported novel Synthesis of alumina Al_xO_y Sub-Microstructure Particles Using In-House Methods. The structure was synthesized from aluminium oxide by in-house prepared method. The synthesis was performed using caustic soda (NaOH) assisted, pure aluminium was dissolved in pre-prepared solution of DI, H_2O_4, NaOH. Al_xO_y was prepared in crucible via different pH solution of DI, H_2O_4, NaOH. The pure aluminium powder was prepared from 2 $NaAl(OH)_4$. The process passed through three reactions; Oxidation $Al(OH)_y$, evaporation Al_xO_y, and dissolution $2NaAl(OH)_{z:}$. The average diameter of the alumina Al_xO_y sub-microstructures between 10.34 to 40.2μm were realised, The gel was washed until no more sulfate ions were detected in the washings.

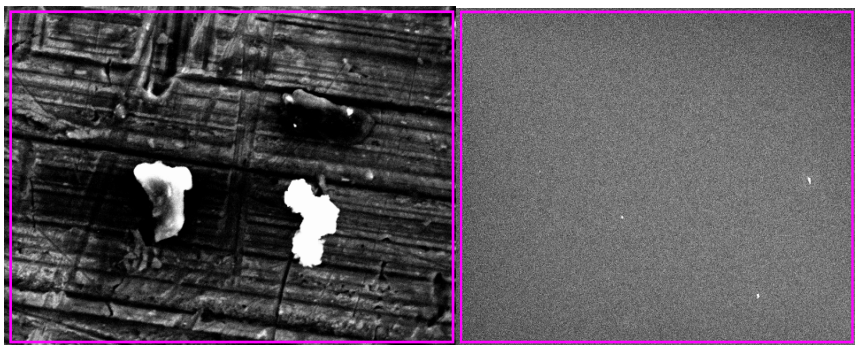

(a) (b)

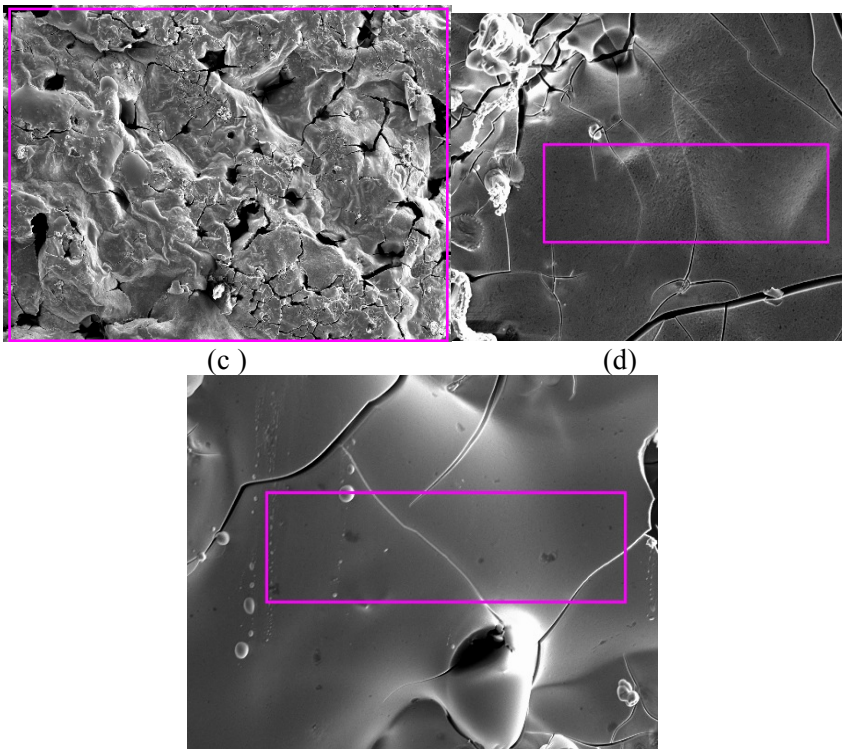

(c) (d)

(e)

Figure 1. SEM images of prepared solution of dissolved Al at different pH contents (a) at 4, (b) at 5, (c) at 6, (d) at 8, (e) at 9

Finally, they were dried at 80 ◦C for 6 h, then ground and passed through a 60-mesh sieve. The samples were then calcined (burn) for 3h in a muffle furnace, in air, at a heating rate of 2 ◦C min^{-1}. Finally activated alumina was obtained.The prepared alumina via the pure aluminum (99.9% pure) reaction was observed during proves. shown the bubbles raising during the reaction, from the fig. 1b , the bubbles settle down at room temperature, with a aqueous NaOH in a reactor to produce a solution of sodium aluminate ($NaAlO_2$). This solution was passed through filter paper and the clear filtrate was neutralized with H_2SO_4, to pH 4, 5,6 8 and 9, resulting in the precipitation of a white gel, Al(OH)3·XH2O. The gel was washed until no more sulfate ions were detected in the washings which were observed in figure 3 and 4. Finally, they were dried at 80 ◦C for 6 h, then ground and passed through a 60 mesh sieve .The samples were then steadily calcined (burn) to removed other unwanted for 3h in a muffle furnace, in air, at a heating rate of 2 ◦C min^{-1}.

3. Results and Discussion

The section presents the result of investigation, the morphology of AL_xO_y sub mirco structures using FESEM. Figure. The figure revealed homogenous distribution of spherical microstructures 2 all the pH values, its shows FE-SEM images of AL_xO_y sub mirco structures with the different aluminium contents. in figure 1 (a),(b),(c),(d) and (e) the results exhibit a homogeneous size and surface morphology over the whole pH values, as can be seen with uniform sizes in each samples. Figure 2 (a) ,(b) and (c) AL_xO_y sub mirco structures, with averages size of 30µm were displayed with uniform distribution with total compact, and densely packed physical observation can be seen. The as synthesis of AL_xO_y sub mirco structures at lower pH values yields a larger, granular microstructure with quite uniform distribution. In the other hand, as the pH value increased, it shows decrease in the micro size size of AL_xO_y sub mirco structures with increasing of pH from 8 to p, which shows an decrease in micro sizes. The measured micro sizes are (a) at 4, ~50µm (b) at 5, 40µm (c) at 6, 20µm (d) at 8, 10µm (e) at 9 shown < ~ 1µm. Shows decreased in the microsize of AL_xO_y sub mirco structures nanostructures with decreasing pH concentration. It is interesting to note that the as the size the aspect

ratio the microstructures increases. A likely explanation for this behaviour is that the enhanced reactivity of pH values increase as compared to lower which results in more rapid dissolution and solubility increase with formation inter ion exchange and subsequent kinetics-driven growth. Although there is a large different of size using on and FE-SEM, image from low pH to high pH but both all concentration yield trends of homogeneity. It is well known that the potential of activated to used in application such as water treatment depends on the micro size of the absorber layer, therefore, the smaller isize are required for the efficient water treatment.

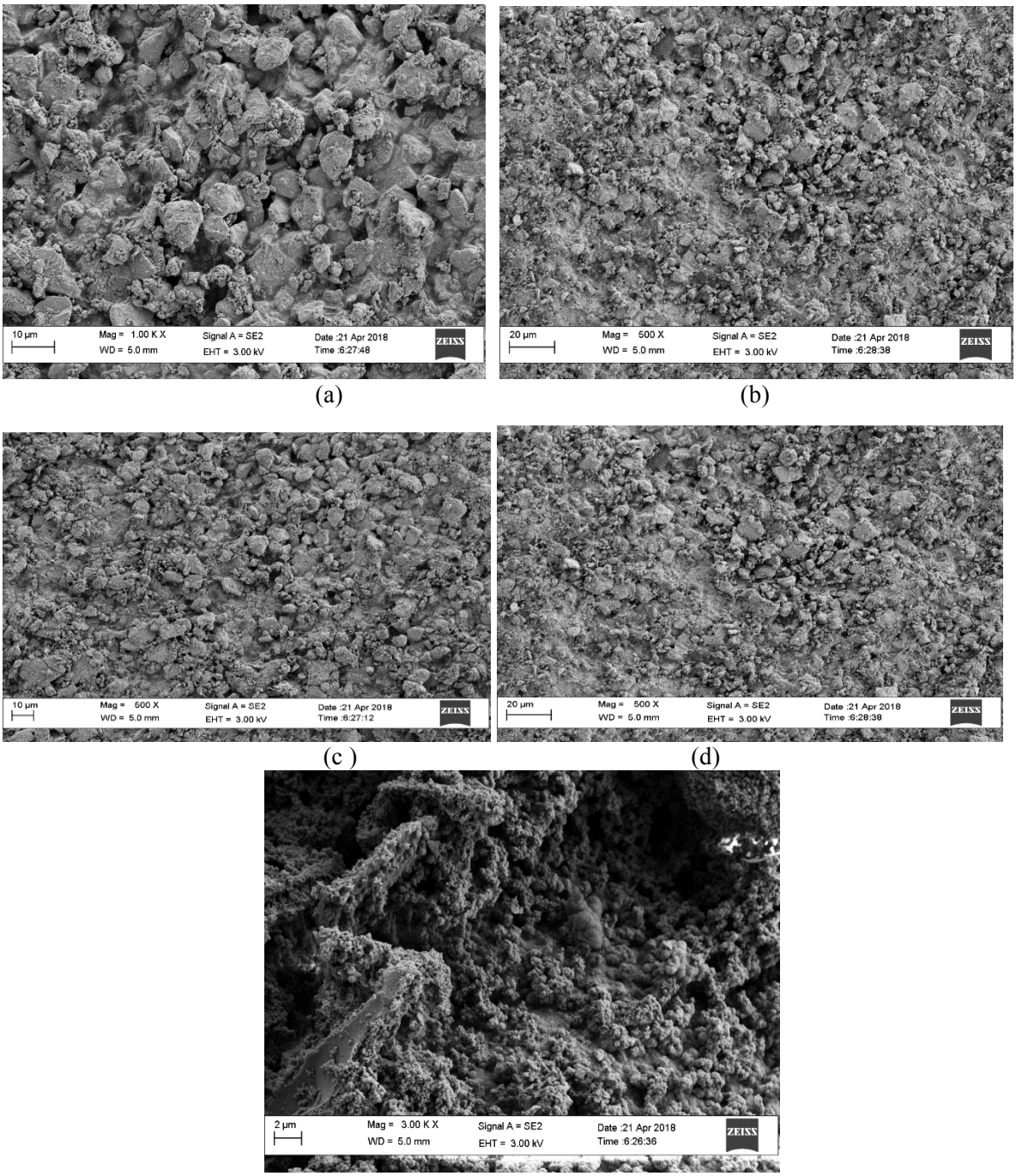

Figure 2. FE-SEM images of synthesised sub-microstructure at different pH contents (a) at 4, (b) at 5, (c) at 6, (d) at 8, (e) at 9

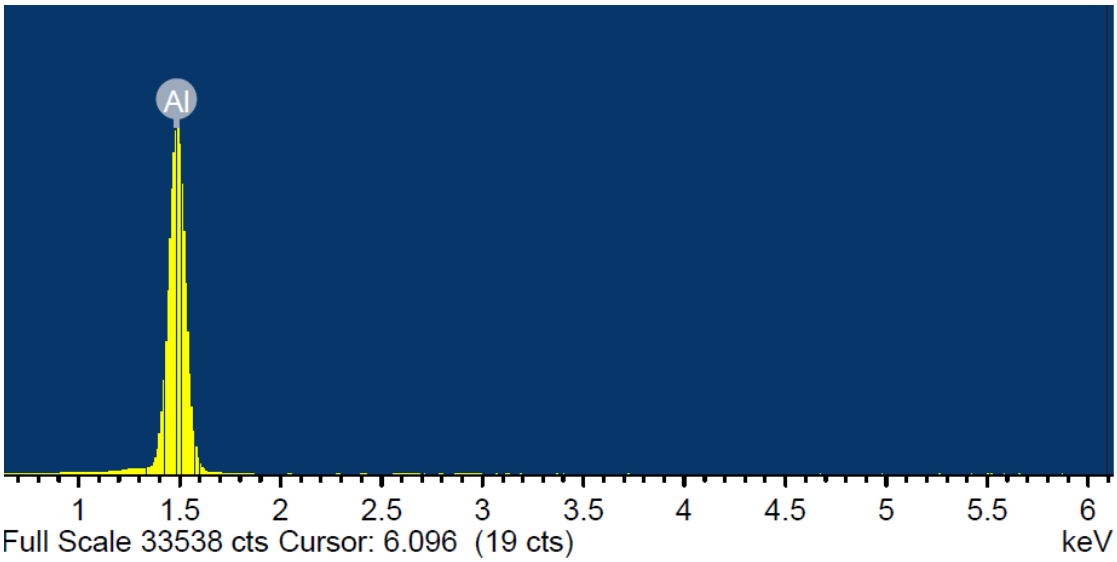

Figure 3. EDX spectra of prepared alumina

To understand the materials, spectrum analysis is conducted using energy dispersion x- rays on active alumina. As can be seed here EDX spectrum shows that the existence of pure aluminum without the inherent oxygen (oxide) and chloride. normally there aluminum native carries oxide. This is due to the diffusion between the oxide layers which is located underneath the alumina naturally. When the diffusion takes place, the oxygen may exist. An investigated was equally conducted on the present of prepared alumina structures based on EDX. It can be observed the peak is high it illustration of it purity of the alumina structures. The alumina exhibits a homogeneous size over the whole substrate, uniform distribution of the might be expected on structures since show only 1 peak as can be observed, this what equally reveled by the FE-SEM images. Moreover, The EDX shown from pyramid shape distribution, the typical peak in the energy dispersion emphasizing the similar crystal nature and grain sizes. The entire spectra were obtained after observed in the region comprised of bands assigned to the pure region to alumina. The peak are shown between three energy region 1 keV, 1.5 keV , 2keV stretching of alumina-alumina bond and grain distribution. The ion stretching region is particularly useful for elucidating alumina-bonding patterns. The confirmation of FTIR result which appeared in in our publication (Rabia et al, 2018). Where at wave numbers between 1000 and 3500 cm-1 the intensities decreased due to the washing total removal of the impurities. This peak has been assigned to the asymmetrical stretching of alumina. As the washing of sulfate ions was done, the Fourier transport infra-red spectra (FTIR) in shown in figure 2, the typical peak in the EDX spectra were obtained after observed in the region comprised of bands assigned to the pure region to alumina. In the paper, the peaks are shown 3376.5cm^{-1}, 1645cm^{-1}, 1096.22cm^{-1}, 1422 cm^{-1} and 1030 cm^{-1} this indicate that alumina getting pure and stretching of alumina-alumina bond exist which correspond to peak at the energy 1 to 2 keV. The ion stretching region is particularly useful for elucidating alumina-bonding patterns. The typical peak for pure alumina is expected between 1000 and 3500 cm-1 the intensities decreased due to the washing. This peak has been assigned to the asymmetrical stretching of alumina.

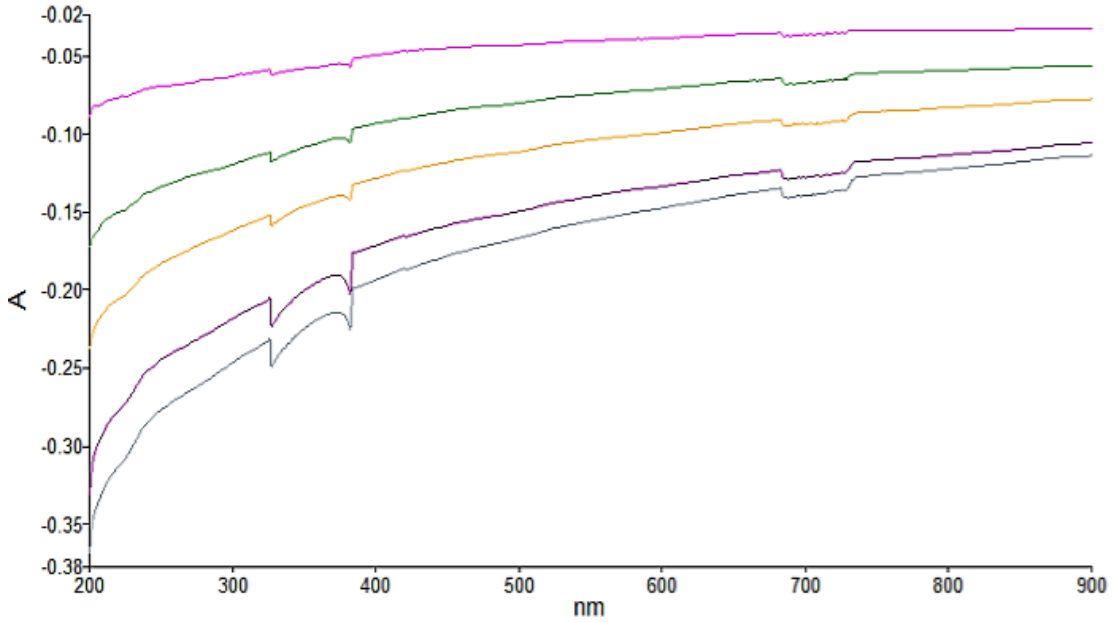

Figure 4. MIR curves sub-microstructure at different pH contents (a) at 4, (b) at 5, (c) at 6, (d) at 8, (e) at 9

The MIR curve shown in Figure for response where the intensity sub-microstructure at different pH contents (a) at 4, (b) at 5, (c) at 6, (d) at 8, (e) at 9. It means that the intensity of MIR is proportional to the number of phone emitted by increasing pH values. The higher energy is dominated by surface state recombination and low energy emission originates from the quantum confinement effect. Furthermore, the energy band gap (E_g) is calculated using. Where λ is the wavelength in (nm). The peak position λmax and the full width of half maximum (FWHM) of the band gap are shifted with increasing pH in linearly to higher wavelength side

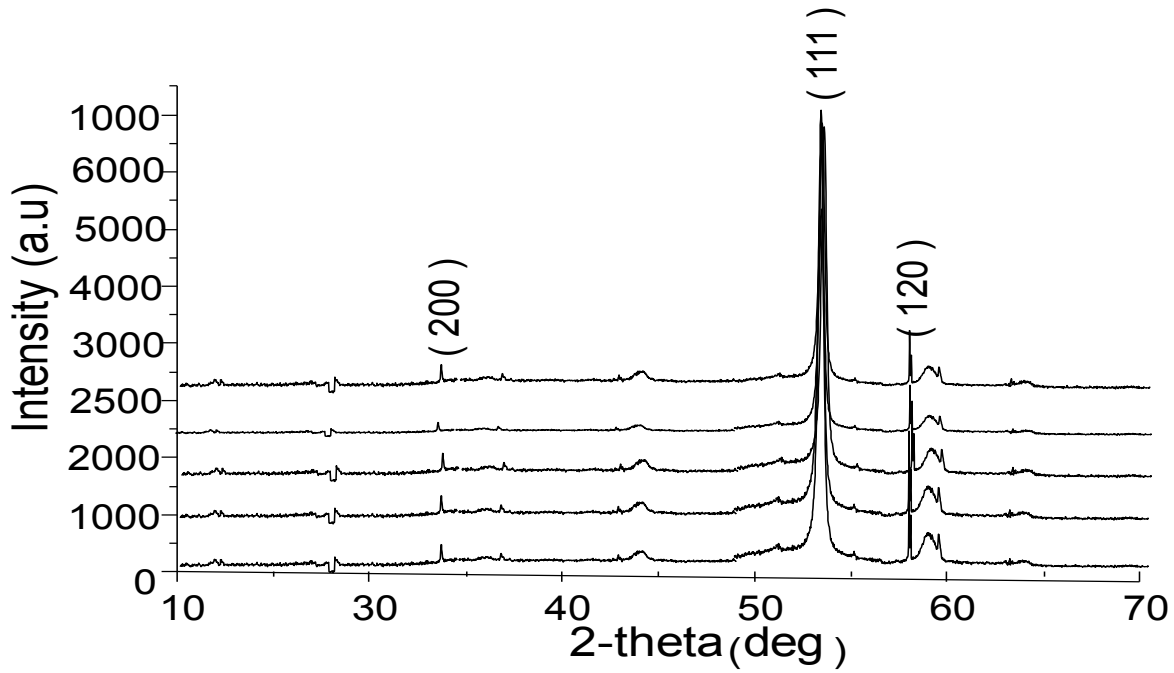

Figure 5. XRD spectra of sub-microstructure at different pH contents (a) at 4, (b) at 5, (c) at 6, (d) at 8, (e) at 9

Figure 5 shows the XRD patterns of the sub-microstructure different pH values of 4, 5 , 6 , 9 , and 9. First of all, the obvious main peaks observed in all of the samples which locate at 2θ = 54.55 and 59.3 which can be attributed to the (200) , (111) and (120) planes of the radial phase of sub-microstructure. It is important to note that the X-ray diffraction patterns of sub-microstructure nanocrystals over the entire composition range show no additional peaks corresponding to secondary impurities such, and also other closely related cation-ordered orthorhombic structures of sub-microstructure. The intensity of the (111) peak becomes more intense and sharp, with the increase of pH, the diffraction peaks monotonously shifts towards small angles indicating that the lattice constant increases. The expansion of lattice constant is attributed to base and acid ion radius is large. Figure5shows the XRD patterns of the ZnO after washed different water flow rate. Generally can be observed that main peaks observed in the sample which locate at 2θ = 18.76, 23.51 and 33.885 which can be attributed to the active alumina bond at xyz, (100) and (200) crystal planes of the alumina active phase of alumina. It is important to note that the X-ray diffraction patterns of alumina particle over the entire purification range show no additional peaks exist for corresponding to secondary impurities such as sulfate ions and also other closely related cation-ordered orthorhombic structures of other elements such radicals. The intensity of the 35 peak becomes more intense and sharp, with the increase wash rate, the diffraction peaks monotonously shifts towards small angles as can be observed indicating that the lattice constant increases which in other attributed for being getting pure.

4. Conclusion

The paper reported novel Synthesis of alumina AlxOy Sub-Microstructure Particles Using In-House Methods. The structure was synthesized from aluminium oxide by in-house prepared method. The synthesis was performed using caustic soda (NaOH) assisted, pure aluminium was dissolved in pre-prepared solution of DI, H2O4, NaOH. AlxOy was prepared in crucible via different pH solution of DI, H2O4, NaOH. The pure aluminium powder was prepared from 2 NaAl(OH)4. The process passed through three reactions; Oxidation Al(OH)y, evaporation AlxOy, and dissolution 2NaAl(OH)z The average diameter of the alumina AlxOy sub-microstructures between 10.34 to 40.2µm were realised. It was found that the high the pH concentration, the smaller the micro structure where pH of 9 has produced AlxOy Sub-microstructure of average diameter ~1µm.

5. Reference

[1]. Abdul Rashid, J. I., Abdullah, J., Yusof, N. A., Hajian, R., Abdul Rashid, J. I., Abdullah, J. Hajian, R. The Development of Silicon Nanowire as Sensing Material and Its Applications. Journal of Nanomaterials, 1–16 (2013).

[2]. Ahmed, R. A., & Fekry, A. M. Preparation and characterization of a nanoparticles modified chitosan sensor and its application for the determination of heavy metals from different aqueous media. International Journal of Electrochemical Science, 8(5), 6692–6708 (2013)..

[3]. Boken, J., & Kumar, D. Detection of Toxic Metal Ions in Water Using SiO 2 @ Ag Core-Shell Nanoparticles, 4(4), 303–308 (2014).

[4]. Chen, K. I., Li, B. R., & Chen, Y. T.. Silicon nanowire field-effect transistor-based biosensors for biomedical diagnosis and cellular recording investigation. Nano Today. Elsevier Ltd. https://doi.org/10.1016/j.nantod.2011.02.001 (2011)

[5]. Ewa Szatyłowicz, Iwona Skoczko (2018) The Use of Activated Alumina and Magnetic Field for the Removal Heavy Metals from Water,Journal of Ecological Engineering , 2018; 19(3):61–67

[6]. ARMAN SEDGHI, NASTARAN RIAHI-NOORIb,, NASER HAMIDNEZHAD and MOHAMMAD REZA SALMANI (2014) Effect of chemical composition and alumina content on structure and properties of ceramic insulators, Bull. Mater. Sci., Vol. 37, No. 2, April 2014, pp. 321–325

[7]. Gralik G. Chinelatto A. Chinelatto L., A. S. A. (2014) Effect of different sources of alumina on the microstructure and mechanical properties of the triaxial porcelain, Cerâmica 60 (2014) 471-481

[8]. Wei Li, Richard Harrington, Yuanzhi Tang, James D. Kubicki, Masoud Aryanpour§, Richard J. Reeder, John B. Parise and Brian L. Phillips (2011) Differential Pair Distribution Function

Study of the Structure of Arsenate Adsorbed on Nanocrystalline γ-Alumina, *Environ. Sci. Technol.*, 2011, 45 (22), pp 9687–9692

[9]. Salvador F., N. Martin-Sanchez, R. Sanchez-Hernandez, M.J. Sanchez-Montero, C. Izquierdo, Regeneration of carbonaceous adsorbents. Part I: Thermal Regeneration, Microporous Mesoporous Mater. 202 (2015a) 259–276.

[10]. Salvador F., N. Martin-Sanchez, R. Sanchez-Hernandez, M.J. Sanchez-Montero, Regeneration of carbonaceous adsorbents. Part II: Chemical, micrbobiological and vacuum regeneration, Microporous Mesoporous Mater. 202 (2015b) 277–296.

[11]. Saka, C., 2012. BET, TG–DTG, FT-IR, SEM, iodine number analysis and preparation of activated carbon from acorn shell by chemical activation with ZnCl2. Journal of Analytical and Applied Pyrolysis, Volume 95, p. 21–24.

[12]. Shah, I. K., Pre, P. & Alappat, B., 2014. 'Effect of thermal regeneration of spent activated carbon on volatile organic compound adsorption performances'. Journal of the Taiwan Institute of Chemical Engineers, Volume 45, p. 1733–1738.

[13]. Xin-hui 2012 Regeneration of microwave assisted spent activated carbon: Process optimization, adsorption isotherms and kinetics. Chemical Engineering and Processing: Process Intensification, Volume 53, p. 53– 62.

[14]. Eliassi A M. Ranjbar (2014) Application of Novel Gamma Alumina Nano Structure for Preparation of Dimethyl ether from Methanol, Int. J. Nanosci. Nanotechnol., Vol. 10, No. 1, Mar. 2014, pp. 13-26

[15]. Michael A. Karakassides, Dimitrios Gournis, Athanasios B. Bourlinos, Pantelis N. Trikalitis and Thomas BakascMagneti (2016) Fe2O3–Al2O3 composites prepared by a modified wet impregnation method, J. Mater. Chem., 2003, 13, 871–876

[16]. Ramana Reddy P., Ajith K. M. and N. K. Udayashankar (2016) Contact angle measurement studies on porous anodic alumina membranes prepared using different electrolytes, Adv. Mater. Lett. 2016, 7(5), 398-401

[17]. Karthikeyan' G, B V Apparao And S Meenakshi, defluoridation properties of activated alumina (2014) 2nd international workshop on fluorosis prevention and defluoridation of water, pp 79-82

[18]. Tijjani Adam U. Hashim and Th S. Dhahi, Silicon nanowire formed via shallow anisotropic etching, Si-ash-trimming for specific DNA and electrochemical detection, Chinese Physics B Vol. 24, No. 6 (2015) 06810

[19]. Tijjani Adam, U Hashim, Design and fabrication of micro-mixer with short turns angles for self-generated turbulent structures, Microsystem Technologies, 1-8, 2015

[20]. T Adam, U Hashim, TS Dhahi, KN Khor, PS Chee, PL Leow, ELECTROCHEMICAL ETCHING: An Ultrasonic Enhance Method of Silicon Nano Porous Fabrication, Wulfenia Journal 20 (1), 45-55, 2013

[21]. Tijjani Adam, H Uda, M Eaqub, PL Leow, The electroosmosis mechanism for fluid delivery in PDMS multi-layer microchannels, American Scientific Publishers All rights reserved.2013

[22]. U Hashim, T Adam, J Lung, P Ling, Fabrication of Microchannel and Micro Chamber for Microfluidic Lab-on-Chip.Australian Journal of Basic & Applied Sciences 7 (1)2013

[23]. T Adam and U. Hashim Light Observation in Polymer: A Study of Silicon-Based Organic Polymer Using Visible Spectroscopy, Australian Journal of Basic and Applied Sciences 7 (1), 76-80, 2013.

[24]. U Hashim, MW Al-Mufti, T Adam, Silicon Nanowire Geometry: Investigation of Interaction Site Potential in Semiconductor-DNA Interaction, Australian Journal of Basic and Applied Sciences 7 (5), 242-245, 2013

[25]. MW Al-Mufti, U Hashim, T Adam, Simulation of Nano lab on chip devices by using COMSOL MultiphysicsJournal of Applied Sciences Research 9 (2), 1056-1061, 2013

[26]. T Adam, U Hashim, KL Foo, TS Dhahi, T Nazwa, Technology development for nano structure formation: Fabrication and characterization, Advanced Science Letters 19 (1), 132-137, 2013

[27]. T Adam, U Hashim, PL Leow, KL Foo, PS Chee, Selection of optimal parameters in fabrication of poly (dimethylsiloxane) microfluidics using taguchi method, Advanced Science Letters 19 (1), 32-36,2013

[28]. T Adam, U Hashim, KL Foo, Microfluidics design and fabrication for life sciences application, Advanced Science Letters 19 (1), 48-53, 2013

[29]. T Adam, U Hashim, ME Ali, PL Leow, The electroosmosis mechanism for fluid delivery in PDMS multi-layer microchannel, Advanced Science Letters 19 (1), 12-15, 2013